Available online at www.sciencedirect.com
SCIENCE DIRECT®
Journal of Catalysis 225 (2004) 439–452
JOURNAL OF CATALYSIS
www.elsevier.com/locate/jcat

Reaction network of steam reforming of ethanol over Ni-based catalysts

Athanasios N. Fatsikostas and Xenophon E. Verykios *

Department of Chemical Engineering, University of Patras, GR-26504 Patras, Greece

Received 27 January 2004; revised 29 April 2004; accepted 29 April 2004

Available online 28 May 2004

Abstract

The reaction of steam reforming of ethanol over nickel catalysts supported on γ-Al_2O_3, La_2O_3, and La_2O_3/γ-Al_2O_3 is investigated employing transient and steady-state techniques. It is found that ethanol interacts strongly with alumina on the surface of which it is dehydrated at low temperatures, and less strongly with lanthana on the surface of which it is both dehydrogenated and dehydrated. Cracking reactions are also observed on the carriers at intermediate temperatures. In the presence of Ni, catalytic activity is shifted toward lower temperatures. In addition to the above reactions, reforming, water–gas shift, and methanation contribute significantly to product distribution. Carbon deposition is also a significant route. It is found that the rate of carbon deposition is a strong function of the carrier, the steam-to-ethanol ratio, and reaction temperature. The presence of lanthana on the catalyst, high steam-to-ethanol ratio, and high temperature offer enhanced resistance toward carbon deposition.

Keywords: Ethanol reforming; Hydrogen production; Nickel catalyst; Lanthana carrier; Transient kinetics

1. Introduction

In recent years, hydrogen—in combination with fuel cells—has been proposed as a major energy source which could contribute toward two goals: reduction of atmospheric pollution and greenhouse gas emissions, and reduction of global dependency on fossil fuels. Until all technical problems related to storage and transportation of hydrogen are resolved, its generation is expected to be accomplished on site by reformation of various gaseous or liquid feedstocks. Biomass-derived materials, or bio-fuels, are viable alternatives for this purpose since they offer high-energy density and ease of handling, so that they can be used for on-demand production of hydrogen for automotive and distributed power generation. An important advantage of bio-fuels for hydrogen production is related to the fact that their use is neutral or nearly neutral with respect to CO_2 emissions. Among the various liquid bio-fuels, ethanol is very attractive as it is produced renewably from many biomass sources, it has relatively high hydrogen content, and it is nontoxic and easy to store and transport. Thus, the use of bio-ethanol as hydrogen carrier for fuel cell applications has a great potential for contributing significantly toward short-to-medium-term targets of energy supply, environmental protection, and regional development.

Hydrogen production from ethanol via steam reforming, catalytic partial oxidation, or autothermal reforming has been the subject of several recent studies [1–8]. The process has been shown to be entirely feasible from a thermodynamic point of view [9–11] and several catalysts have been proposed which show sufficient activity and stability to be further considered for practical applications [12–19]. Although many metals have been shown to be active in this process, Ni seems to be the preferred active ingredient. As we have shown in previous work [1,6], Ni dispersed on La_2O_3 offers a catalyst for steam reforming of ethanol which is not only active and selective toward hydrogen production but also stable with time on stream, even under conditions which favor carbon formation and deposition.

In the present study, the interaction of ethanol with the surface of catalyst carriers (γ-Al_2O_3, La_2O_3, and La_2O_3/γ-Al_2O_3) and Ni catalysts employing these carriers is investigated using transient techniques. From these studies as well as from steady-state experiments, the reaction network of the steam reforming of ethanol is investigated with respect to homogeneous gas-phase reactions, reactions taking place on

* Corresponding author.
E-mail address: verykios@chemeng.upatras.gr (X.E. Verykios).

0021-9517/$ – see front matter
doi:10.1016/j.jcat.2004.04.034

the carriers, and reactions taking place on the metal, at different temperatures.

2. Experimental

2.1. Catalyst preparation and characterization

The Ni catalysts employed in the present study were prepared by the wet impregnation method of the carriers (La_2O_3, γ-Al_2O_3, La_2O_3/γ-Al_2O_3) using $Ni(NO_3)_2$ (Alfa Products) as the metal precursor. Commercial γ-Al_2O_3 (Engelhard) and La_2O_3 (Alfa Products) were used, while La_2O_3/Al_2O_3 was prepared by wet impregnation of γ-Al_2O_3 (Engelhard) with lanthanum nitrate (Alfa Products). The solid residue was calcined in air at 900 °C for 30 h. The La_2O_3 content of the carrier was 10% by mass. Further details of the preparation methods are described elsewhere [1]. The BET surface areas of the fresh materials and after calcination at 900 °C for 30 h appear in Table 1. The apparatus used was a Micromeritics Gemini III 2375 surface analyzer. Metal dispersion of fresh catalysts was also determined by hydrogen chemisorption employing a modified Fisons Instruments (Sorptomatic 1900) apparatus. Uptake of H_2 at monolayer coverage of the Ni particles was obtained by extrapolation of the linear portion of the adsorption isotherm to zero pressure. Metal dispersion deriving from these measurements is also shown in Table 1.

2.2. Apparatus

Both transient and steady-state experiments were carried out in an apparatus which consists of a flow switching system, a heated reactor, and an analysis system. The flow apparatus has been described in detail elsewhere [20]. The reactor consists of two 6.0-mm o.d. sections of quartz tube, which serve as inlet and outlet to and from a quartz cell of 8.0-mm o.d. (6-mm i.d.). The total length of the reactor is 15.0 cm. The catalyst sample, approximately 100 mg, of particle size between 0.18 and 0.25 mm, was placed in the cell and kept in place by means of quartz wool. This configuration resulted in a catalytic bed of approximately 8–9 mm in length.

Table 1
BET surface areas of fresh and calcined materials and Ni dispersion of fresh catalysts

Material	BET surface area ($m^2\,g^{-1}$)		Metal dispersion of fresh catalyst (%)
	Fresh	After calcination at 900 °C/30 h	
Al_2O_3	180	62.9	
La_2O_3	3.9	–	–
La_2O_3/Al_2O_3	97.1	–	–
Ni/Al_2O_3	117.9	62.9	3.1
Ni/La_2O_3	12.3	2.0	1.1
$Ni/(La_2O_3/Al_2O_3)$	68.2	44.8	3.6

The temperature of the catalyst was measured along the catalyst bed by means of a K-type thermocouple placed within a quartz capillary well, which ran through the bed. Heating of the reactor was provided by an electric furnace controlled by a programmable controller. The gas composition at the reactor outlet was continuously monitored by an on-line quadrupole mass spectrometer (Fisons, SXP Elite 300 H) connected to the reactor via a heated silicon capillary tube of 2 m length. The pressure in the main chamber was UHV level ($\approx 10^{-7}$ mbar). Calibration of the mass spectrometer signal was performed based on prepared mixtures of precisely known composition. For all experiments—transient or steady state—gas-phase composition was calculated from the mass spectrometer signal at m/e ratios of 44, 43, 40, 32, 31, 28, 26, 15, 2 for CO_2, CH_3CHO, Ar, O_2, CH_3CH_2OH, CO, C_2H_4, CH_4, and H_2, respectively. Fragmentation of the different species was calibrated and contributions from other than the indicated ones were subtracted, as well as the background level.

2.3. Experimental procedure

2.3.1. Adsorption/desorption of ethanol (TPD)

Prior to any experiment, all samples were reduced in situ using H_2 flow (40 cc min^{-1}) at 700 °C for approximately 1 h. After purging with He for 15 min, the sample was cooled under He flow to room temperature (22 °C). At this point, 40 cc min^{-1} of a mixture consisting of 1% CH_3CH_2OH in He was directed into the reactor chamber for 20 min in order to saturate the catalyst surface with ethanol. Adsorption was followed by purging with He for 15 min so as to clean all lines. After this treatment, temperature programmed desorption (TPD) was initiated, in which temperature was increased with a linear rate of $\beta = 15$ K min^{-1}, while the sample was maintained under He flow (ca. 50 cc min^{-1}).

2.3.2. Temperature-programmed surface reaction (TPSR)

The TPSR experiment is basically a TPD experiment carried out under reactive conditions. The pretreatment procedure was identical with that of the TPD experiment. After pretreatment of the material, adsorption of one of the reactants at room temperature for 20 min took place, the surface was then purged with He for 15 min, and then the other reactant (1% in He) was passed over the saturated surface in a temperature-programmed manner, using the same linear heating rate ($\beta = 15$ K min^{-1}).

2.3.3. Temperature-programmed reaction

After in situ reduction of the catalyst at 700 °C, He purging and cooling to room temperature, a mixture containing 1% EtOH and 2% H_2O in He was directed through the catalyst bed at a rate of 44 cc min^{-1} while temperature was ramped from 25 to 750 °C with a linear rate of 15 K min^{-1}. The reactor effluent was continuously monitored by the mass spectrometer, as described above. Mass spectrometer signals of reactants and products were converted to concentration by

calibration with similar mixtures of precisely known composition.

2.3.4. Titration of deposited carbon

Temperature-programmed oxidation (TPO) experiments were conducted in order to estimate the amount of carbon deposited on the catalytic surface. TPOs were conducted in a similar manner as described above, following steady-state reactions for a period of 2 h under various experimental conditions. During reaction, the catalyst was exposed to an ethanol–water (1% EtOH/1% or 1.5% or 2% water, balance He) mixture at a total flow of 44 cc min^{-1}, at temperatures of 600, 700, or 750 °C. After purging with He at 700 °C for 15 min and cooling to room temperature, TPO with 1% O_2/He was initiated with a heating rate of 15 K min^{-1}.

The reproducibility of transient experiments was checked by performing identical experiments on the same as well as on different catalyst batches. In all cases identical results were observed.

3. Results and discussion

3.1. TPD of adsorbed ethanol

The interaction of ethanol with the surface of the carriers (γ-Al_2O_3, La_2O_3, and La_2O_3/Al_2O_3) and the catalyst (Ni dispersed on the above carriers) was investigated by adsorption of ethanol on these materials, followed by temperature-programmed desorption. Adsorption took place at atmospheric temperature by a flow of 1% ethanol in He over the solids for approximately 20 min. The lines were cleaned by a flow of pure He for 5 min, prior to initiation of a linear temperature ramp, at a rate of 15 K min^{-1}. The temperature ramp was stopped at 750 °C and this temperature was maintained for approximately an additional 15 min.

The TPD spectrum obtained over the La_2O_3 carrier, following the procedure described above, is shown in Fig. 1a. It is apparent that very weak signals are observed, which is due to the fact that the surface of La_2O_3 absorbs only small quantities of ethanol, probably due to the low specific surface area of the carrier. Ethanol desorbs molecularly, at very low rate, at temperatures up to 450 °C. Within the same temperature range, small quantities of acetaldehyde, hydrogen, and CO are discernible, while ethylene peaks at about 320 °C. These species originate from dehydrogenation, dehydration, and cracking reactions. Above 500 °C, CO_2 seems to be the main species desorbing. CO_2 probably originates from decomposition of carbonates formed during the adsorption/decomposition of ethanol [21], or from other species and fragments adsorbed on the surface of the carrier [22–24].

Addition of 20% Ni on the La_2O_3 carrier results in an entirely different TPD spectrum (Fig. 1b). Nickel leads to fast decomposition of absorbed ethanol, as witnessed by the appearance of H_2, CH_4, and, to a smaller extent, CO peaks at temperatures below 100 °C, according to

$$C_2H_5OH \leftrightarrows CH_4 + CO + H_2. \quad (1)$$

Hydrogen peaks at about 150 °C, while, a new reaction route emerges at about 200 °C. The only detectable product is hydrogen, pointing toward dehydrogenation of ethanol with concomitant adsorption or fast decomposition of acetaldehyde according to

$$C_2H_5OH \leftrightarrows C_2H_4O + H_2, \quad (2)$$

$$C_2H_4O \leftrightarrows CH_4 + CO. \quad (3)$$

CO and CO_2 emerge at about 300 °C and peak at about 450 °C. The lack of significant hydrogen evolution at the CO/CO_2 peak temperature may imply that CO and CO_2 are formed from carbonaceous deposits on the Ni surface and oxygen species originating either from the carrier or from adsorbed species. It is interesting to note that no decomposition of carbonates ($T > 600$ °C) is observed, which may be attributed to competition between the Ni and the La_2O_3 surfaces for different reaction routes. Such competition may prevent significant formation of lanthanum carbonates.

The TPD spectrum obtained over the Al_2O_3 carrier, following the adsorption procedure described earlier, is shown in Fig. 1c. A very large ethanol desorption peak at about 100 °C dominates the spectrum. This is due to the large adsorption capacity of Al_2O_3. In competition with ethanol desorption, ethanol dehydration,

$$C_2H_5OH \leftrightarrows C_2H_4 + H_2O, \quad (4)$$

and cracking [reaction (1)] take place at low temperatures. Dehydration of adsorbed ethanol is significantly more apparent at higher temperatures, peaking at about 250 °C. The origin of CO in the 200–300 °C temperature range, the spectrum of which follows that of ethylene, is not clear. A possible route may be the partial decomposition of adsorbed fragments via the action of lattice oxygen.

The identical TPD experiment conducted over the 20% Ni/Al_2O_3 catalyst produces a very different spectrum (Fig. 1d). This spectrum is also significantly different than that produced over the 20% Ni/La_2O_3 catalyst (Fig. 1b), noting that the scale differs by approximately one order of magnitude. At low temperatures (< 100 °C), three processes seem to compete, namely desorption of adsorbed ethanol, its cracking producing CH_4, CO, and H_2 [reaction (1)], and, to a very small extent, dehydrogenation producing acetaldehyde [reaction (2)]. CO is not eluting into the gas phase at this temperature probably because it interacts strongly with the metal, as observed earlier with TPD experiments over the same catalysts [22]. Based on Fig. 1c, C_2H_4 [originating from ethanol dehydration on Al_2O_3, reaction (4)] would also be expected in this temperature range. Its absence indicates that ethylene is reacting fast on the metal surface or it is deposited in the form of polymeric species on to the carrier surface. Similar but more intense activity is taking place in the temperature range between 200 and 300 °C. In this temperature range the desorption of ethanol is weakened while

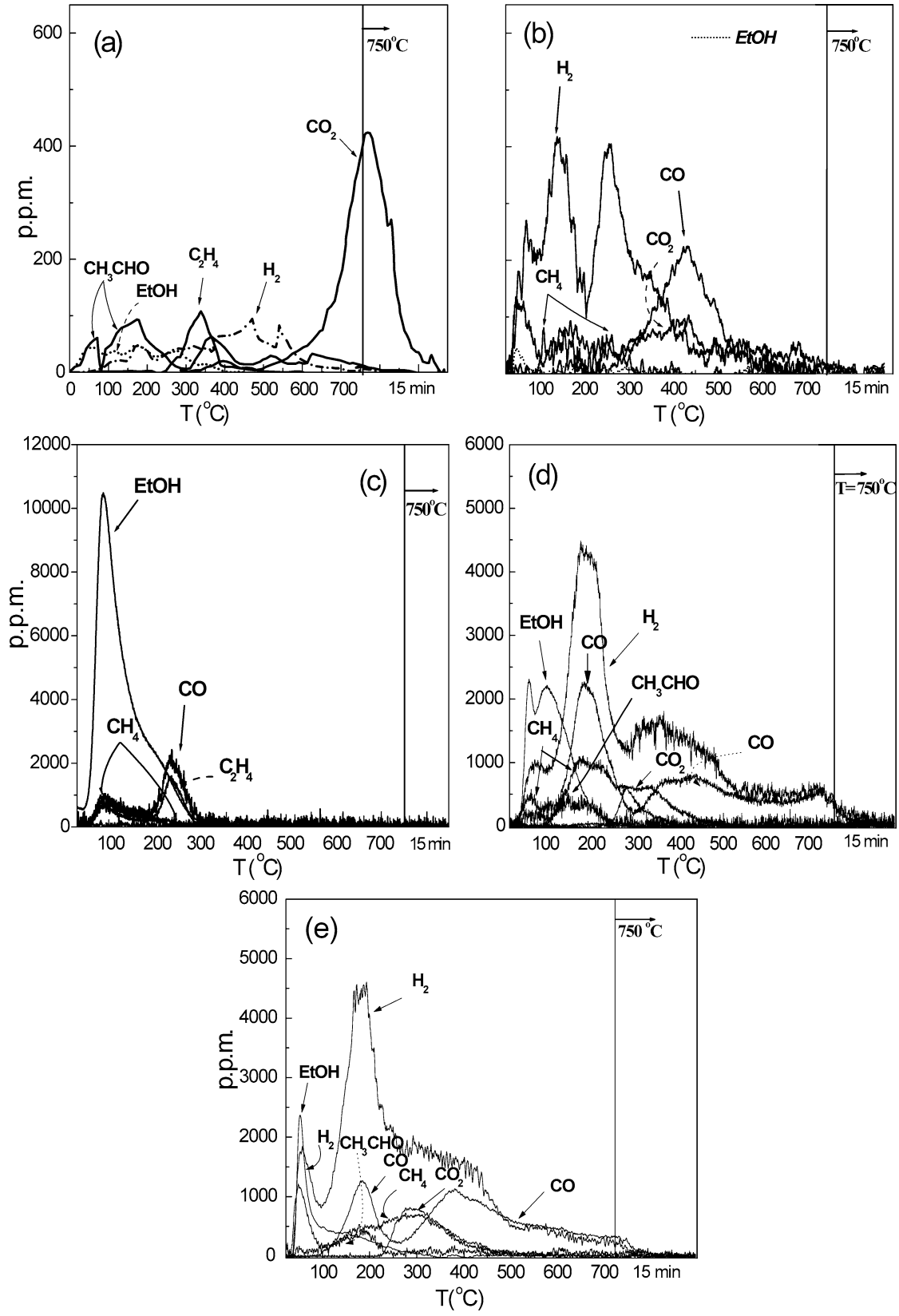

Fig. 1. TPD spectra obtained following room temperature ethanol adsorption from an 1% EtOH in He mixture on: (a) La_2O_3; (b) 20% Ni/La_2O_3; (c) γ-Al_2O_3; (d) 20%Ni/γ-Al_2O_3; (e) 20%Ni/(La_2O_3/γ-Al_2O_3). Experimental conditions: flow rate of adsorption mixture, $F_T = 40$ cc min^{-1}; mass of catalyst, 100 mg; $\beta = 15$ K min^{-1}; $P = 1$ atm.

Table 2
Carbon balance of transient experiments

Catalyst	TPD of adsorbed EtOH	TPSR		TP reaction
		Preadsorbed ethanol	Preadsorbed water	
None	–	–	–	4
La_2O_3	10	–	–	27
Al_2O_3	16	–	–	36.5
La_2O_3/Al_2O_3	–	–	–	40
Ni/La_2O_3	48.5	–	–	6
Ni/Al_2O_3	40.7	–	–	–
$Ni/(La_2O_3/Al_2O_3)$	24.1	14.4	18.8	11.4

dehydrogenation and cracking reactions [reactions (1) and (3)] dominate. The CO peak is very large because it contains CO produced at lower temperatures, which had been retained on the catalyst surface and it is desorbing at elevated temperatures. The water–gas shift (WGS) reaction becomes important at temperatures above 250 °C, producing CO_2:

$$CO + H_2O \leftrightarrows CO_2 + H_2. \quad (5)$$

The Boudouard reaction,

$$2CO \leftrightarrows CO_2 + C, \quad (6)$$

may be adding to the observed CO_2 in this temperature range, while the methanation reactions,

$$CO + 3H_2 \leftrightarrows CH_4 + H_2O, \quad (7)$$

$$CO_2 + 4H_2 \leftrightarrows CH_4 + 2H_2O, \quad (8)$$

are adding to the observed CH_4 signal. Most activity seems to cease above 500 °C. Residual H_2 and CO desorb from the surface, or they may be produced from decomposition of strongly adsorbed surface species.

The TPD spectrum over the 20% $Ni/(La_2O_3/Al_2O_3)$ catalyst is shown in Fig. 1e. It is observed that, at low temperatures, the presence of lanthana on the carrier hinders dehydration of ethanol while promoting the route of dehydrogenation which produces large quantities of hydrogen and CO, the latter being produced from fast decomposition of acetaldehyde on Ni. This is probably due to the fact that La_2O_3, a basic molecule, has been adsorbed on the acidic sites of Al_2O_3, which are primarily responsible for dehydration. Apart from that, the two spectra are very similar. As will be discussed in a subsequent section, a significant role of lanthana is to enhance the stability of the catalyst with time on stream.

The overall carbon balance of the TPD experiments is shown in Table 2. The carbon balance is poor, indicating that significant quantities of carbon deposit onto the catalysts during the TPD experiment. This is expected, primarily at the low temperature range, which thermodynamically and kinetically favors carbon deposition. Over the carriers (Al_2O_3 and La_2O_3) the carbon deficit is better, probably due to the low overall activity of these materials.

3.2. Temperature-programmed surface reactions over the $Ni/(La_2O_3/Al_2O_3)$ catalyst

The reaction of steam reforming of ethanol was investigated by TPSR of preadsorbed ethanol or water, over the $Ni/(La_2O_3/Al_2O_3)$ catalyst. In the first set of experiments, ethanol was preadsorbed on the catalyst surface at room temperature by flow of an 1% EtOH in He mixture, followed by purging with He for 3 min and subsequent flow of an 1% H_2O/He mixture, while a temperature ramp of 15 K min^{-1} was applied. The resulting TPSR spectrum is shown in Fig. 2a. This spectrum is qualitatively similar to the TPD spectrum (Fig. 1e) but it also has significant differences. At low temperatures, the presence of steam in the gas phase seems to promote desorption of adsorbed ethanol and thus prevention of its decomposition on the surface. This is probably due to displacement of ethanol from the surface by competitive adsorption of water, indicating that both molecules compete for the same adsorption sites on the carrier. The spectrum is characterized by two large hydrogen peaks at 180 and 300 °C, the first one is accompanied by CO evolution while the second one by CO_2 evolution. In addition, CH_4 also appears in the gas phase at about 250 °C while small quantities of acetaldehyde evolve over a wide temperature range. The first H_2 peak is due to dehydrogenation of ethanol. Apparently, most of the acetaldehyde produced remains in the adsorbed state, while a fraction decomposes according to reaction (3), producing CO and CH_4 which appear between 120 and 220 °C. Decomposition of adsorbed ethanol and/or acetaldehyde at higher temperatures (> 220 °C) results in the appearance of H_2 and CH_4. CO_2 probably originates from CO, produced by ethanol decomposition [reaction (1)], and/or acetaldehyde decomposition [reaction (3)] or acetaldehyde steam reforming,

$$C_2H_4O + H_2O \leftrightarrows 2CO + 3H_2, \quad (9)$$

followed by the WGS reaction [reaction (5)].

Reactions leading toward carbon deposition on the catalyst surface [reaction (6)] and

$$C_2H_4 \rightarrow \text{ polymeric deposits (coke)} \quad (10)$$

may be also operable under the present experimental conditions.

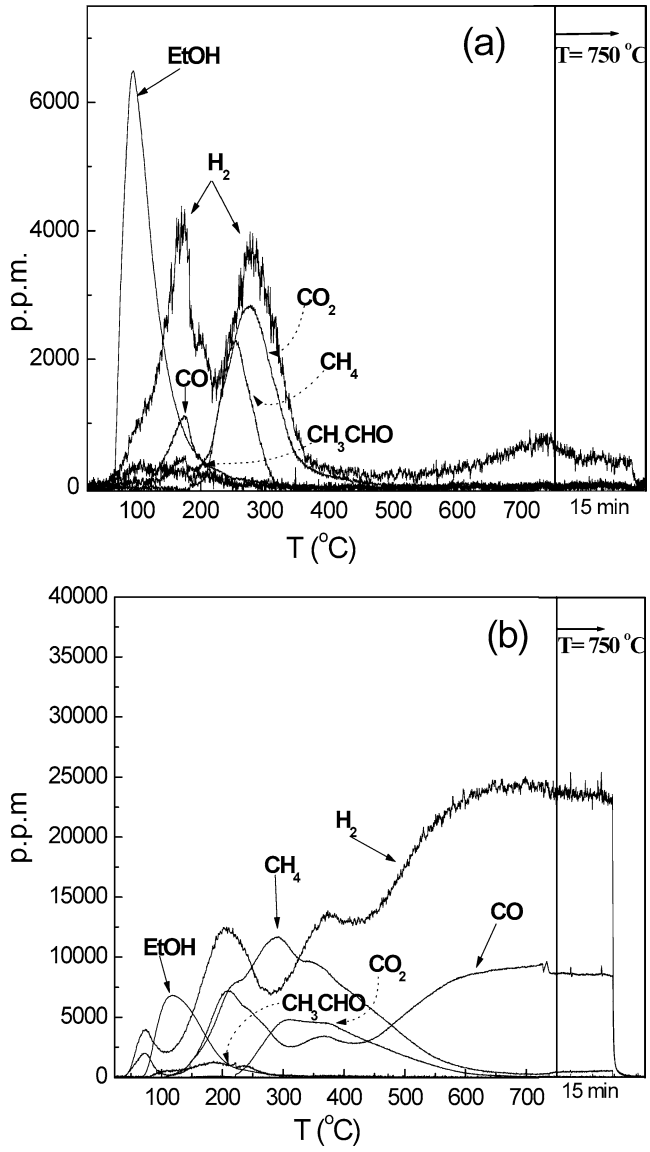

Fig. 2. Temperature-programmed surface reactions over the 20% Ni/(La_2O_3/Al_2O_3) catalyst. (a) Ethanol is preadsorbed onto the catalyst. Steam (1% H_2O/He) flows over the bed while temperature is ramped with a linear rate of 15 K min^{-1}. (b) Steam is preadsorbed on the catalyst. Ethanol (1% EtOH/He) flows over the bed while temperature is ramped at the same rate.

The reverse TPSR procedure was performed in order to examine the behavior of the system when H_2O is preadsorbed on the catalytic surface, followed by flow of 1% EtOH/He mixture and linear temperature ramp. The resulting spectrum is presented in Fig. 2b. The presence of preadsorbed steam on the catalyst surface seems to enhance the chemistry of the system (note that the scale in Fig. 2b is about five times larger than that of Fig. 2a). Ethanol adsorbs on the surface at temperatures below 70 °C, while simultaneously decomposing to H_2, CO, and CH_4 [reaction (1)]. Above this temperature, ethanol desorbs to the gas phase while it continues to decompose and to dehydrogenate producing acetaldehyde. The increased concentration of CO relative to CO_2 over the entire temperature range is probably due to the reverse WGS reaction [reaction (5)], which is driven by the low water concentration, especially at elevated temperatures. At temperatures higher than 300 °C, all ethanol which enters the reactor decomposes. Methane also decomposes according to

$$CH_4 \rightarrow 2H_2 + C. \quad (11)$$

It is interesting to note that some of these reactions continue to occur for a period of over 15 min isothermally at 750 °C.

The overall carbon balance of the TPSR experiments is also shown in Table 2. In this case, the carbon balance is satisfactory, indicating that small quantities of carbon are deposited on the catalyst under the present experimental conditions. In the case of preadsorbed ethanol, the high partial pressure of steam over the catalyst at all temperatures prevents carbon deposition or even assists in gasifying deposited carbon at elevated temperatures. In the case of preadsorbed steam, the presence of steam on the surface, especially at low temperatures, weakens the interaction of ethanol with the surface which, in turn, leads to reduced rates of carbon deposition.

3.3. Reaction pathway under transient conditions

The reaction pathway over various materials was investigated as a function of temperature, employing transient experiments in which temperature was ramped linearly from 25 to 750 °C at a rate of $\beta = 15$ K min^{-1} while an ethanol–water mixture of molar ratio EtOH:H_2O = 1:2 (1% EtOH, 2% H_2O, He balance) was flowing at a steady rate (F_T = 44 cc min^{-1}) over the catalyst. Homogeneous reactions were investigated in the same manner employing an empty reactor tube, and the results are shown in Fig. 3a. It is apparent that consumption of ethanol is initiated at about 400 °C and becomes important above 500 °C. The main products are CO, H_2, CH_4, and CH_3CHO, while traces of C_2H_4 are also detected in the gas phase. The signals of CO and CH_4 follow the same trend, indicating that they originate from the C–C bond rupture of CH_3CHO, which is produced by homogeneous dehydrogenation of ethanol. Ethylene is produced at elevated temperatures by homogeneous dehydration of ethanol.

Similar reactions take place in the presence of La_2O_3 in the reactor (Fig. 3b), but they occur at significantly lower temperatures. It seems that ethanol is partially adsorbed up to 300–350 °C, at which temperature dehydration and dehydrogenation reactions take place simultaneously, as evidenced by the signals of acetaldehyde and ethylene. Acetaldehyde decomposes at a high rate while ethylene is significantly more resistant to reactions on the La_2O_3 surface. Reforming reactions dominate at temperatures higher than 600 °C, producing primarily H_2 and CO_2.

Similar spectra obtained over γ-Al_2O_3 are shown on Fig. 3c. Ethanol is totally adsorbed onto the alumina surface at temperatures up to 70 °C. At 200 °C dehydration of adsorbed ethanol [reaction (4)] is initiated, giving rise to

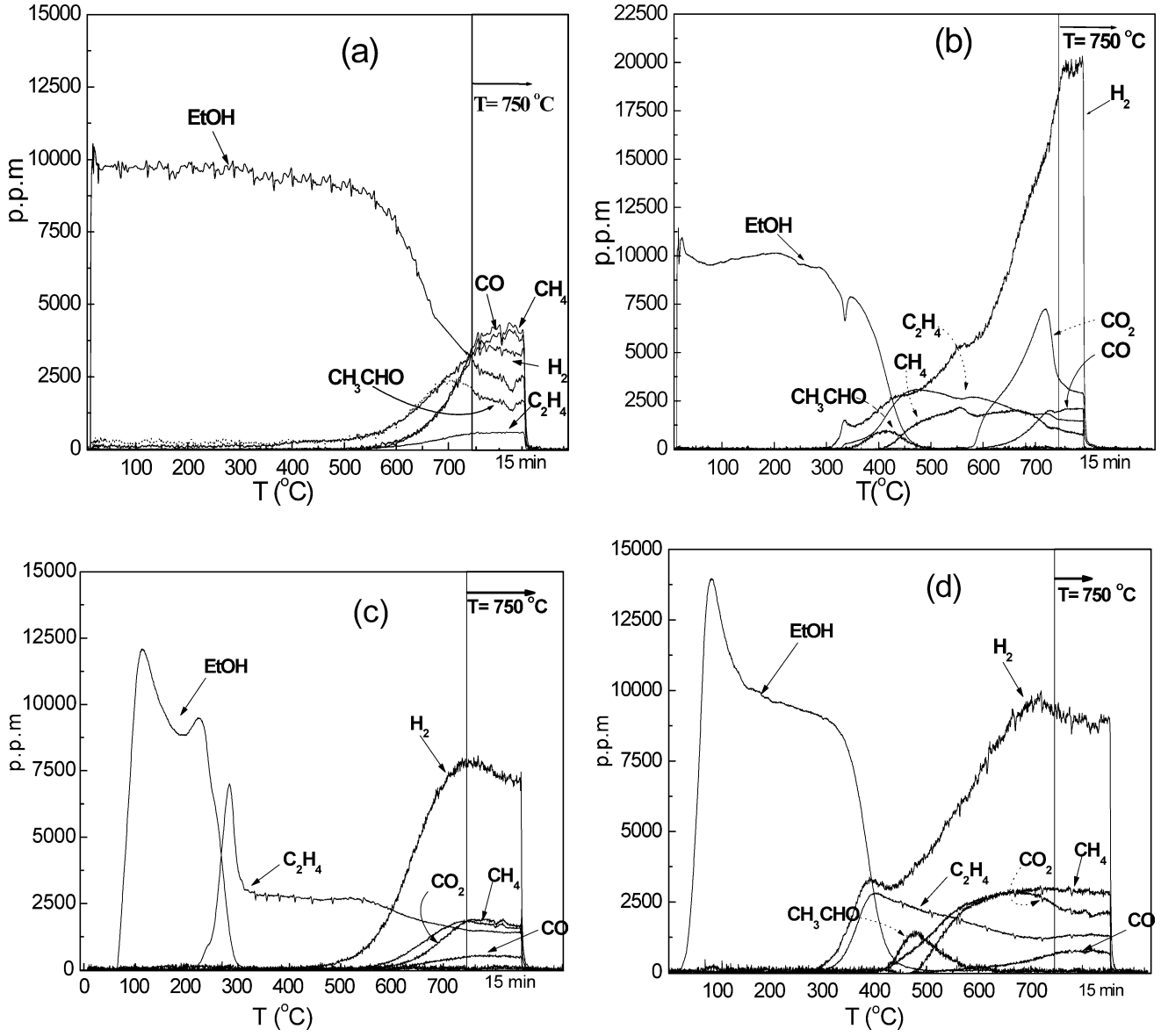

Fig. 3. Temperature-programmed reactions over: (a) empty reactor tube; (b) La_2O_3; (c) γ-Al_2O_3; (d) 10% La_2O_3/Al_2O_3. A mixture containing 1% EtOH and 2% H_2O in He is flown ($F_T = 44$ cc min^{-1}) in the reactor while temperature is ramped at a linear rate of 15 K min^{-1}; mass of catalyst, 100 mg; $P = 1$ atm.

gas-phase ethylene. Ethylene peaks at around 300 °C and a further increase of temperature leads to a decrease of gas-phase ethylene. The sharp decrease of ethylene at 300 °C and the decrease at 600 °C may be attributed to the formation of coke [25] according to reaction (10). It is interesting to note that ethylene is present in the gas phase over the entire duration of the experiment, indicating the difficulty of cracking or reforming of ethylene over alumina. Hydrogen appears in the gas phase at about 500 °C, indicating the initiation of dehydrogenation reaction at this temperature over the acidic sites of alumina, which is probably accompanied by the formation of surface ethoxy species [26,27], which lead to acetaldehyde formation. Acetaldehyde is not detected in the gas phase, as in the case of La_2O_3, as it remains in the adsorbed state. CO, CO_2, and CH_4 appear at temperatures higher than 600 °C, produced from cracking and reforming reactions of ethanol and acetaldehyde. The formation of CO_2 could also be attributed to reaction (5). Methane may also be produced from the hydrogenation of excess carbon at the surface, according to the reverse of reaction (11).

A similar experiment over the La_2O_3/Al_2O_3 carrier produced a spectrum (Fig. 3d), which combines features of the spectra observed over the La_2O_3 (Fig. 3b) and Al_2O_3 (Fig. 3c) carriers. The appearance of acetaldehyde in the gas phase in the temperature range of 400 to 600 °C, in contrast to the case of Al_2O_3 (Fig. 3b), may indicate that La_2O_3 stabilizes acetaldehyde and does not promote decomposition or reforming reactions at intermediate temperatures. Comparison of the two spectra also shows that La_2O_3 promotes

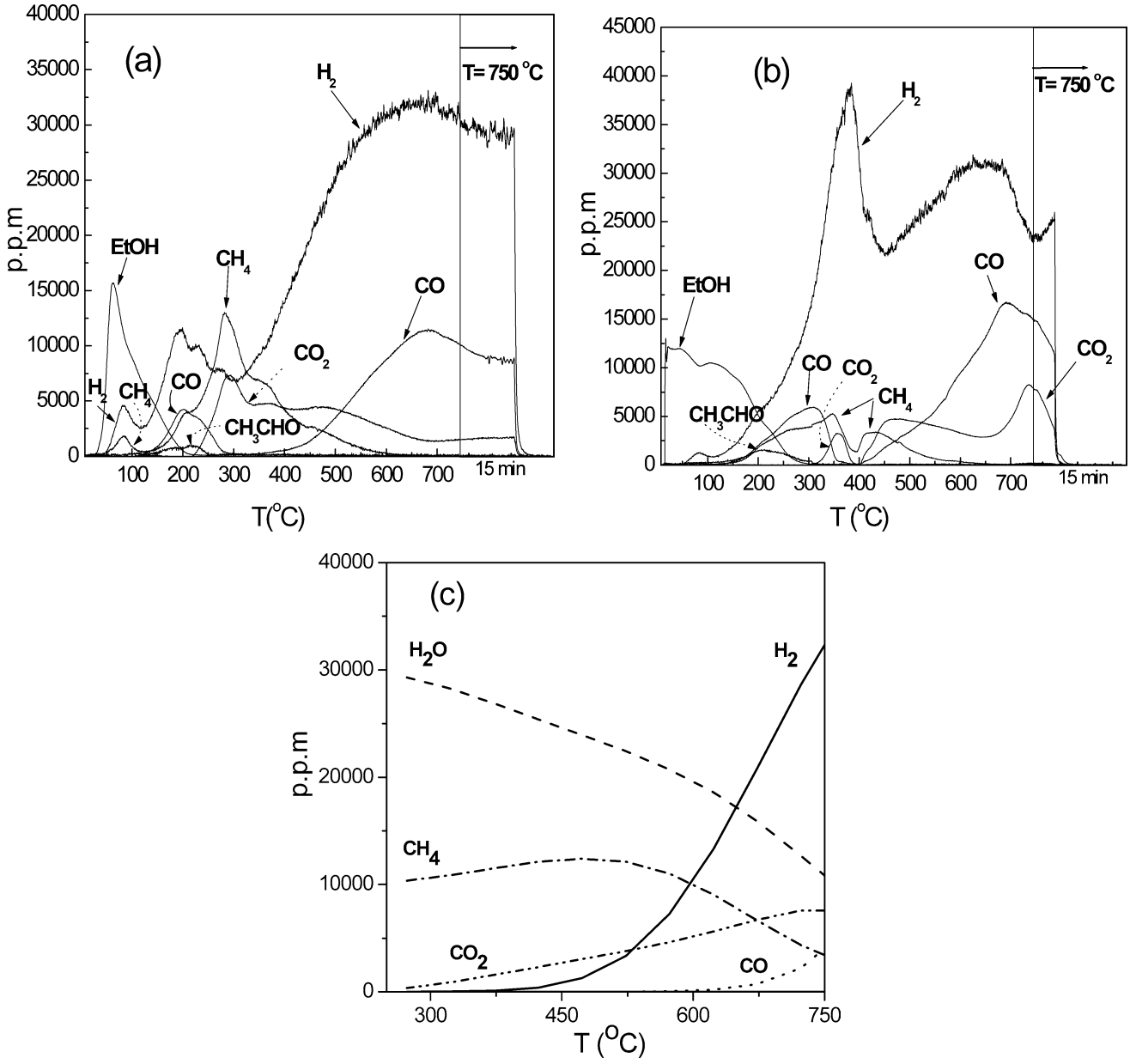

Fig. 4. Temperature-programmed reactions over: (a) 20% Ni/(La_2O_3/Al_2O_3); (b) 20% Ni/La_2O_3 (conditions identical to those of Fig. 3); (c) equilibrium concentrations for a reaction mixture of 1% EtOH and 2% H_2O in He; $P = 1$ atm.

hydrogen formation via dehydrogenation reactions at much lower temperatures, compared to Al_2O_3.

When Ni is deposited on the La_2O_3/Al_2O_3 carrier, the reaction spectrum, under the same experimental conditions, which is shown on Fig. 4a, is drastically different, as compared to that of the carriers. A general characteristic is that there is significantly more catalytic activity, which is now shifted toward lower temperatures. Ethanol decomposes at low temperatures (50–100 °C) to form the C_1 molecules CH_4 and CO as well as H_2 [reaction (1)]. Obviously, nickel favors the C–C bond scission of ethanol and a methyl group is liberated to form methane gas by addition of a hydrogen atom from the surface [26,28]. Ni is also inducing rapid dehydrogenation of ethanol and subsequently rapid decomposition of acetaldehyde to CH_4 and CO [reaction (3)]. As temperature increases, the adsorption of ethanol is completed and, for temperatures between 150 and 200 °C, the dominant reaction is the decomposition of ethanol according to reaction (1).

In the temperature range of 200 to 300 °C, a rapid decrease in the concentrations of CO and H_2 is observed, in addition to the rise of a sharp peak of CH_4 ($T = 280$ °C). This behavior reveals the formation of CH_4 via the methanation reaction [reaction (7)]. Within the same temperature range (215 to 330 °C), a large CO_2 peak appears. It could be attributed to the WGS reaction, but the fact that H_2 does not

increase within the same range suggests that CO_2 formation is related to the Boudouard reaction [reaction (6)]. This reaction may be responsible for significant carbon deposition on the catalyst surface.

At temperatures between 330 and 470 °C, CO_2 production continues at a steady rate, while H_2 production is gradually increased. Methane continues to decrease while CO begins to rise at about 360 °C. The increase of H_2 concentration, in association with the decreasing CH_4 and constant CO_2 formation rates, indicate that the WGS reaction and CH_4 decomposition are the main reactions taking place.

Above 500 °C, H_2 and CO concentrations continue to increase before they become nearly steady at around 600 °C, where CH_4 steam reforming is completed. The CO_2 formation rate is considerably decreased, which is probably due to the reverse WGS reaction. At temperatures above 600–700 °C, steam reforming of ethanol dominates, leading to high CO and H_2 concentrations. It should be noted that CO_2 concentration is significantly less than CO concentration due to the relatively high ethanol-to-steam ratio employed in these experiments ($EtOH/H_2O = 1/2$), which thermodynamically favors the reverse WGS reaction.

The same experiment was also performed over the Ni/La_2O_3 catalyst. The spectrum obtained is shown in Fig. 4b. Some important differences are observed compared to the $Ni/(La_2O_3/Al_2O_3)$ case. First of all, the amount of ethanol adsorbed is very small, due to the reduced specific surface area of La_2O_3, as previously noted. Another difference is the absence of low temperature bond scission of ethanol, which was noted in the case of $Ni/(La_2O_3/Al_2O_3)$ at about 80 °C. On the contrary, a small peak at this temperature in the spectrum of H_2 shows that dehydrogenation of adsorbed ethanol takes place at low temperatures. This is verified by desorption of acetaldehyde, which is initiated at about 100 °C. The behavior of the two catalysts is approximately the same at temperatures between 100 and 200 °C, where ethanol decomposes according to reaction (1). The most significant differences are observed within the temperature range of 200–400 °C: a large peak of H_2 ($T = 380$ °C) accompanied by a smaller one of CO_2 centered at 360 °C, and drastic reduction of CO, can be attributed to the WGS reaction. This hydrogen peak was not observed in Fig. 4a, but, instead, one of CH_4 at about 300 °C, probably due to the methanation reaction.

In order to compare the results of the TP reaction experiments with thermodynamic predictions, equilibrium concentrations were estimated in the temperature range of 300 to 750 °C, under conditions resembling those of the experiments. Results are shown in Fig. 4c. At low temperatures, the equilibrium H_2 concentration is very low, while the methane concentration is appreciable, in direct contrast to the experimental observations. This implies that the methanation reaction is far from equilibrium, as would be expected because of the slow rates induced by low temperatures. At high temperatures, the experimental H_2 and CH_4 concentrations approach those predicted by equilibrium. However, the CO and CO_2 concentrations do not approach equilibrium, while even their tendency is opposite that predicted by thermodynamics, implying that the water–gas shift reaction is far removed from equilibrium under the present experimental conditions.

3.4. Reaction pathway under steady-state conditions

The reaction pathway with respect to temperature was also investigated under steady-state conditions, in a different apparatus, by allowing the reaction to attain steady state before moving to a different temperature. Results obtained with an empty reactor tube (homogeneous reactions) are presented in Fig. 5a. It is apparent that under the present conditions ($F_T = 160$ cc min^{-1}, $EtOH:H_2O = 1:3$) homogeneous activity is initiated at about 600 °C and becomes significant at temperatures higher than 700 °C. Homogeneous activity at low temperatures is primarily toward dehydrogenation, while at higher temperatures dehydration and cracking or dissociation also take place.

Steady-state experiments were also performed in the presence of Ni/La_2O_3 and Ni/Al_2O_3 catalysts. Results of ethanol conversion and product distribution with respect to temperature appear in Fig. 5b and 5c, respectively. When the reactor is loaded with the Ni/La_2O_3 catalyst, activity is initiated at significantly low temperatures. In this case ethanol conversion is observed at temperatures as low as 300 °C and increases drastically with temperature. Essentially complete conversion of ethanol is observed at about 650 °C. As in the case of homogeneous reactions, dehydrogenation is the preferred reaction route at low temperatures. At $T > 550$ °C the only reaction products which are observed are H_2, CO, CO_2, and CH_4, indicating that at higher temperatures product distribution may be dictated by the equilibrium of the water–gas shift and the methanation reactions.

The Ni/Al_2O_3 catalyst presents high activity and selectivity toward hydrogen production at elevated temperatures. As temperature is reduced, significant quantities of ethylene appear in the gas phase. This results in rapid carbon accumulation on the catalyst, loss of its reforming activity, and eventually, at significantly lower temperatures, disintegration of the structural rigidity of the catalyst. Significant pressure drop in the reactor prevents operation at low temperatures (< 550 °C). This is one of the most significant differences between the Ni/La_2O_3 and the Ni/Al_2O_3 catalysts, i.e., their stability with time on stream which stems from different carbon accumulation rates under reaction conditions, especially at lower temperatures.

3.5. Titration of carbon deposited under reaction conditions

One of the major issues of catalytic reforming of hydrocarbons is carbon deposition on the surface and subsequent gradual deactivation of the catalyst. This phenomenon was investigated in the present study by conducting the reaction

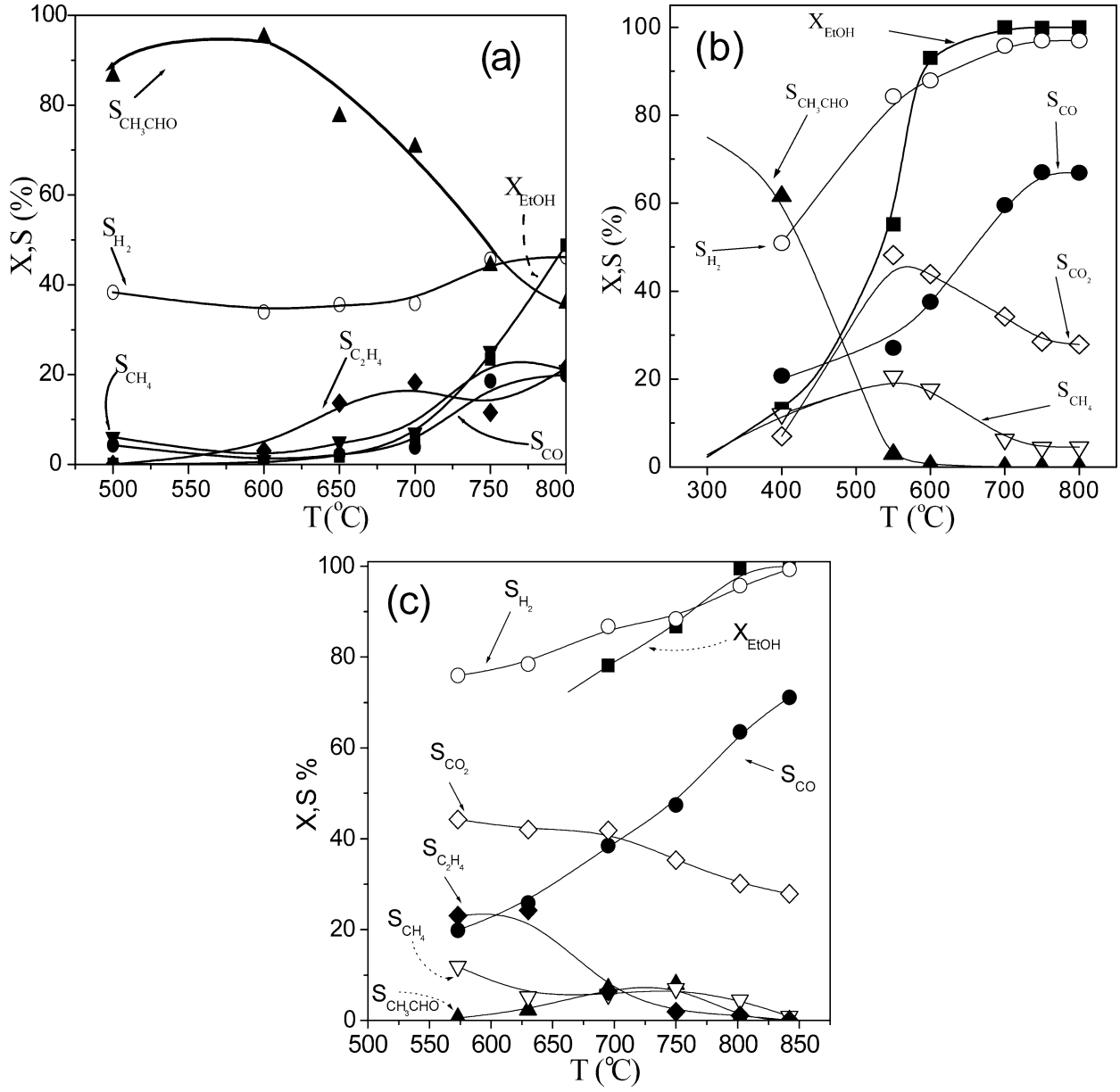

Fig. 5. Ethanol conversion and product distribution under steady-state conditions (40 cc min^{-1} EtOH and 120 cc min^{-1} H_2O) in: (a) empty reactor; (b) 20% Ni/La_2O_3; (c) 20% Ni/Al_2O_3 catalyst; mass of catalyst, 100 mg; $P = 1$ atm.

under steady-state conditions for a period of 2 h, followed by cooling in the presence of He and subsequent exposure of the catalyst to a 1% O_2 in He mixture while the temperature was ramped at a linear rate of 15 K min^{-1} up to 750 °C (TPO). Product evolution during reaction and CO_2 as well as O_2 evolution during the TPO were recorded by mass spectrometry. No CO was detected during the TPO experiments.

Typical reaction and TPO spectra, obtained over the Ni/Al_2O_3 and the $Ni/(La_2O_3/Al_2O_3)$ catalysts, for reaction conducted at 600 °C with a 1% EtOH and 1% H_2O in He mixture, are shown in Fig. 6a and 6b, respectively. In both cases, the main reaction products are H_2 and CO, while smaller quantities of CO_2, CH_4, and CH_3CHO are also observed. In the TPO spectra, there is no direct correlation between the quantity of O_2 consumed and the quantity of CO_2 formed. Oxygen is consumed at low temperatures, before evolution of CO_2 is detected. Apparently, oxygen is used to oxidize the Ni particles, which are in the reduced state under reaction conditions. The surface of the carrier may also be in a somewhat reduced state, thus consuming part of the oxygen. In the case of the $Ni/(La_2O_3/Al_2O_3)$ catalyst (Fig. 6b), part of the oxygen consumed may be attributed to the formation of lanthanum oxalate species [22–24]. At higher temperatures, the evolution of CO_2 corresponds well with the consumption of O_2. In all spectra recorded, two peaks of CO_2 were observed, indicating that there may be two distinct carbon species on the catalyst surface. One of these may be attributed to polymeric carbon originating from ethylene

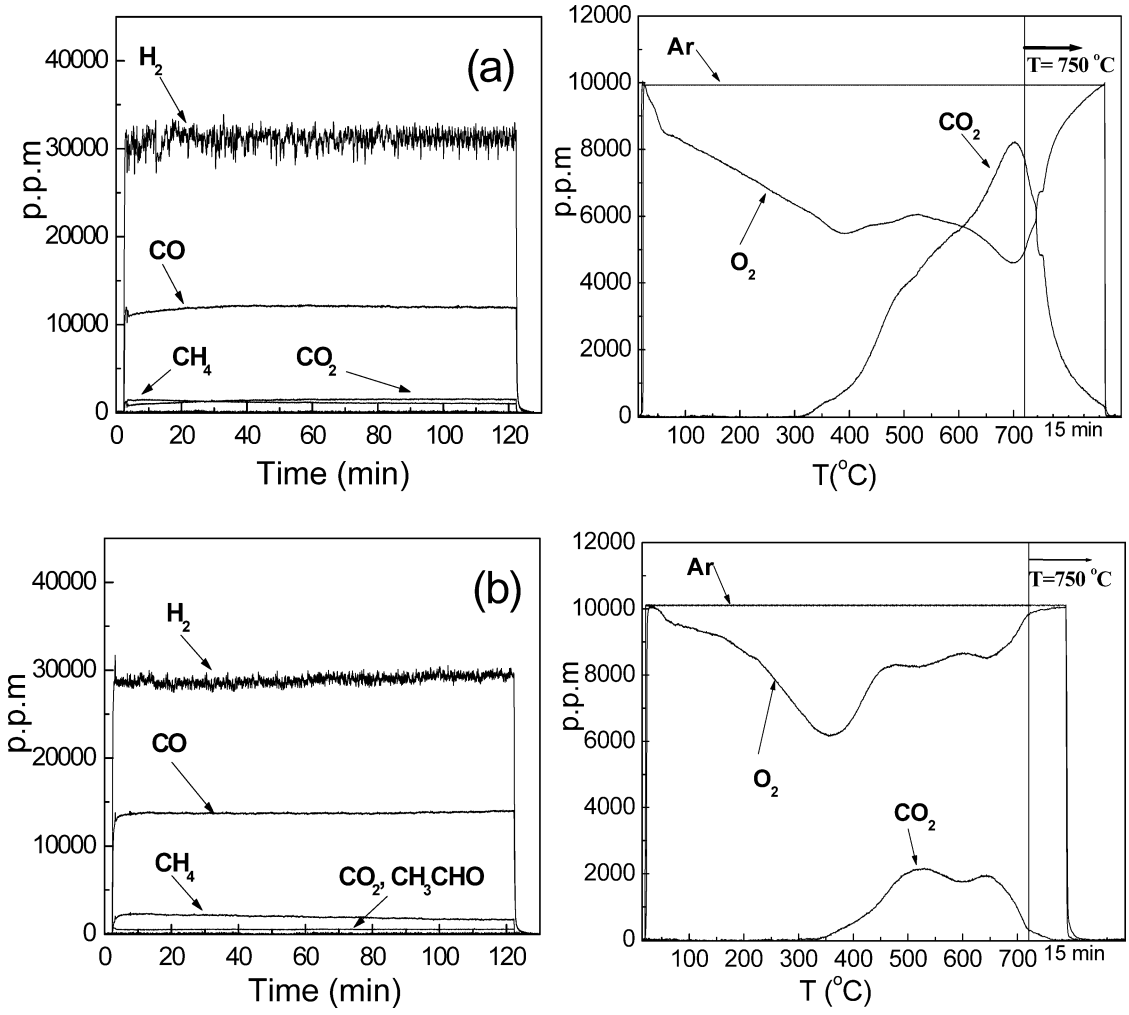

Fig. 6. Product distribution of steady-state experiment conducted for a period of 2 h (1% EtOH and 1% H_2O in He, $T = 600\,^{\circ}C$, $F_T = 44$ cc min^{-1}) and oxygen and CO_2 responses of TPO with mixture 1% O_2/He of carbon deposits on the catalyst during steady-state experiment. Catalyst: (a) 20% Ni/Al_2O_3; (b) 20% Ni/(La_2O_3/Al_2O_3); mass of catalyst, 100 mg; $P = 1$ atm, $\beta = 15$ K min^{-1}.

polymerization while the other one may be attributed to CH_x ($0 < x < 3$) species originating from partial or complete dehydrogenation of C1 molecules. The existence of two peaks in CO_2 production during the temperature-programmed oxidation of coked catalysts samples has been previously reported in the literature [29, and references therein]. It is generally assumed that the lower temperature peak is due to coke deposited on the metal surface while the higher temperature peak (generally the most significant) is attributed to coke deposited on the carrier. The presence of lanthana on the carrier, as, for example, in the Ni/(La_2O_3–Al_2O_3) catalyst, affects both types of accumulated carbon. Its influence on the carrier arises from its adsorption and blocking of acidic sites of Al_2O_3 which promote dehydration and cracking of ethanol with concomitant carbon accumulation. Its influence on the metal can be attributed to the formation of lanthanum oxalate species, as noted before, as well as to the possible partial structure modification to the stable spinel structure of La_2NiO_4 and $NiAl_2O_4$ [30].

Results obtained over different catalysts, under different reaction conditions are summarized in Fig. 7. It must be pointed out that the reaction conditions employed in the present study are rather severe in the sense that they are inductive of carbon formation. This was done so as to accelerate the rate of carbon formation and to be able to estimate the rate of deposition over realistic reaction times. It is shown in Fig. 7a that carbon deposition is strongly influenced by the substrate upon which the Ni active phase is dispersed. This is reasonable since, as it was shown earlier, the substrate itself participates directly in the reaction network. The highest rate of carbon deposition is observed over Al_2O_3. This is due to the fact that Al_2O_3 catalyzes the ethanol dehydration reaction which leads to ethylene formation. Ethylene is further polymerized, leading to significant carbonaceous deposits. When La_2O_3 is dispersed over the Al_2O_3 carrier, the rate of carbon deposition is reduced significantly due to adsorption of basic lanthana species on the acidic sites of Al_2O_3 and subsequent deactivation of these sites which

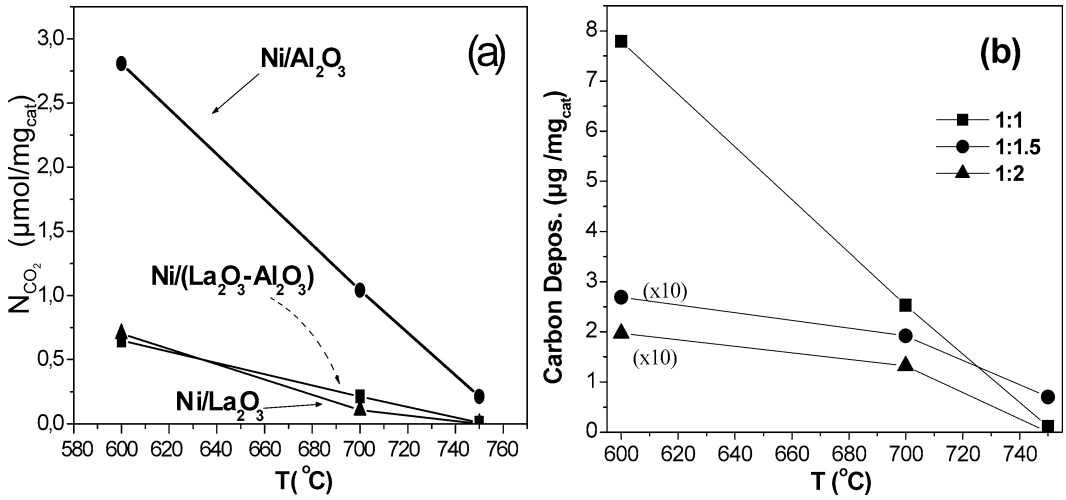

Fig. 7. Quantity of carbon accumulated over a reaction period of 2 h (steady state) at different temperatures: (a) over different catalysts (mixture 1% EtOH and 1% H_2O; $F_T = 44$ cc min^{-1}) and (b) for various EtOH–H_2O ratios over the 20% Ni/(La_2O_3/Al_2O_3) catalyst following 2-h reaction with mixture EtOH/$H_2O = X$, ($X = 1/1$, 1/1.5, 1/2); $F_T = 40$ cc min^{-1}; in all the experiments concentration of ethanol was 1%. Amount of deposited carbon was estimated by TPO with 1% O_2/He; $F_T = 44$ cc min^{-1}; with temperature ramped from 25 to 750 °C; $\beta = 15$ K min^{-1}.

are responsible for the dehydration reaction. The rate of carbon deposition over the Ni/(La_2O_3/Al_2O_3) catalyst is almost identical to that over the Ni/La_2O_3 catalyst, indicating that lanthana is covering a large portion of the alumina, or that all acidic sites of Al_2O_3 are deactivated by adsorption of basic La_2O_3.

As is shown in Fig. 7a, the rate of carbon deposition is also a strong function of reaction temperature, decreasing significantly with temperature. This is due to both thermodynamic as well as kinetic reasons. Thermodynamically, the reactions which lead to carbon formation are not favored at high temperatures. Kinetically, the reactions responsible for carbon removal, such as the reactions of carbon with steam or with CO_2, are favored at higher temperatures. As expected, the rate of carbon deposition is also a strong function of the ethanol-to-steam molar ratio, as shown in Fig. 7b. The amount of carbon deposited over the 2-h reaction period decreases rapidly with increasing the steam content of the reaction mixture since the reaction between deposited carbon and steam is favored. The ethanol-to-steam molar ratios used in the present study are unrealistically high. The stoichiometric ratio of EtOH:H_2O is 1:3. Frequently, lower ratios are employed in practice so as to reduce the rate of carbon deposition.

4. Overall discussion

It is apparent from the results presented in previous sections that the interaction of ethanol with the catalytic materials employed in the present study, both in the presence and absence of steam, leads to a highly complicated reaction network. Certain reactions occur in the gas phase, especially at elevated temperatures, others on the carrier surfaces and still others on the Ni surface. The possibility of interaction between these three domains, in the sense that reaction intermediates produced in one domain react further on other domains, cannot be excluded.

γ-Al_2O_3 seems to promote primarily the dehydration reaction of ethanol, probably via ethoxy or acetate species [31], producing ethylene which leads to polymeric carbonate species, at relatively low temperatures. On the other hand, La_2O_3 seems to promote primarily the dehydrogenation reaction and, to a smaller extent, the dehydration reaction. Dehydrogenation leads to acetaldehyde which decomposes rapidly to CH_4 and CO. When both materials (γ-Al_2O_3 and La_2O_3) are used as catalyst carriers in the form of mixed oxide, a combination of catalytic properties is observed. Thus, dehydration and dehydrogenation reactions compete over a large temperature range. It should also be noted that La_2O_3, a basic material, may be adsorbing on the acidic sites of γ-Al_2O_3, thus reducing the dehydration activity of the latter. Thus, in the La_2O_3–Al_2O_3 carrier, the dehydrogenation reaction competes favorably with the dehydration reaction, although the surface area of Al_2O_3 is significantly higher than that of La_2O_3 (Table 1).

In the presence of nickel, the catalysts become significantly more active, as indicated by the shift of conversion to lower temperatures. Pure nickel, as Yates and co-workers [26,28] have shown, causes bond breaking of ethanol in the following order: O–H, –CH_2–, C–C, and –CH_3. Therefore, it should be assumed that the key reaction for all catalysts tested at temperatures up to 300 °C is the dehydrogenation of ethanol to surface adsorbed CH_3CHO_{ads}. The following scheme seems to describe best the transformations of CH_3CHO_{ads} at this temperature range:

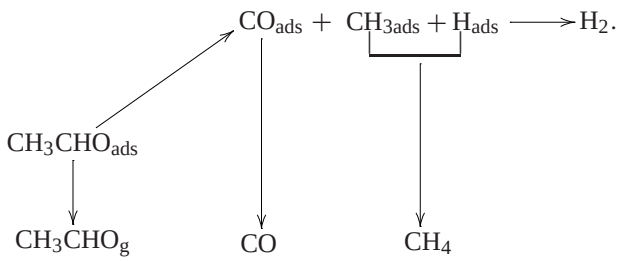

In the presence of Ni, because of its high dehydrogenation activity, the contribution of the carrier is primarily in the dehydration route. In general, dehydration leads to carbon deposits on the catalyst surface. Significant carbon deposits have been observed on the catalysts containing Al_2O_3, indirectly from the carbon balances (Table 2) and directly in steady-state experiments (Fig. 7). Carbon may be deposited through either a surface route which can lead to polymeric species, as predicted by Guisnet and Magnoux [29] in a recent investigation of the chemistry of coke formation, or through decomposition of ethylene [32].

Titration of carbon deposits under reaction conditions reveals their dual nature and the ability of lanthana to inhibit formation of graphitic carbon on the catalytic surface. The low temperature coke can be assumed to be formed by polymeric species originating from ethylene. The second form of coke is attributed to dehydrogenated methyl groups formed onto the carrier, in addition to carbon originating from the Boudouard reaction. It is generally believed [32,33] that due to the dissociation of CO on Ni, carbon diffuses into the bulk between the metal particles and the carrier, where it creates carbon islands consisting of graphitic carbon. Due to the fact that this kind of coke is rather inactive, its accumulation results in deactivation and even disintegration of the catalyst. The beneficial effect of lanthana is that it constrains the adsorbed C, and, via lanthanum oxycarbonates, it combusts it to CO [22,23], thus hindering the creation of the above-noted carbon islands.

5. Conclusions

The following conclusions can be drawn from the results of the present study:

(1) Catalyst carriers such as Al_2O_3 and La_2O_3 interact strongly with ethanol at relatively low temperatures. Al_2O_3 promotes dehydration and cracking while La_2O_3 primarily promotes dehydrogenation and cracking.
(2) The presence of Ni active phase on the catalyst shifts activity toward lower temperatures. Ni promotes reforming of ethanol and acetaldehyde as well as the water–gas shift and methanation reactions.
(3) The overall reaction network of ethanol steam reforming is highly complicated and, at elevated temperatures, results in the formation of H_2, CO, CO_2, and traces of CH_4. Carbon also deposits and accumulates on the catalyst surface.
(4) In presence of alumina, carbon deposition occurs at a very high rate, resulting from ethylene polymerization. Impregnation of Al_2O_3 with La_2O_3 results in a significantly reduced rate of carbon deposition.
(5) The rate of carbon deposition is favored at low reaction temperatures and under high ethanol-to-steam ratios.

Acknowledgments

This work was funded in part by the Commission of the European Union under Contract NNE5-1999-00272 and by the General Secretariat of Research and Technology of Greece under the PENED program.

References

[1] A.N. Fatsikostas, D.I. Kondarides, X.E. Verykios, Catal. Today 75 (2002) 145.
[2] F. Mariño, E. Cerrella, S. Duhalde, M. Jobbagy, M. Laborde, Int. J. Hydrogen Energy 23 (1998) 1095.
[3] F. Mariño, M. Boveri, G. Baronetti, M. Laborde, Int. J. Hydrogen Energy 26 (2001) 665.
[4] V. Galvita, G. Semin, V. Belyaev, V. Semikolenov, P. Tsiakaras, V. Sobyanin, Appl. Catal. A 220 (2001) 123.
[5] V. Klouz, V. Fierro, P. Denton, H. Katz, J. Lisse, S. Bouvot-Mauduit, C. Mirodatos, J. Power Sources 105 (2002) 26.
[6] A.N. Fatsikostas, D.I. Kondarides, X.E. Verykios, Chem. Commun. (2001) 851.
[7] L.D. Schmidt, G.A. Deluga, in: AIChE Annual Meeting, San Francisco, November 16–21, 2003.
[8] G.A. Deluga, J.R. Salge, L.D. Schmidt, X.E. Verykios, Science 303 (2004) 993.
[9] E. Garcia, M. Laborde, Int. J. Hydrogen Energy 16 (1991) 307.
[10] K. Vasudeva, N. Mitra, P. Umasankar, S. Dhingra, Int. J. Hydrogen Energy 21 (1996) 13.
[11] I. Fishtik, A. Alexander, R. Datta, D. Geana, Int. J. Hydrogen Energy 25 (2000) 31.
[12] F. Haga, T. Nakajima, H. Miya, S. Mishima, Catal. Lett. 48 (1997) 223.
[13] S. Cavallaro, S. Freni, Int. J. Hydrogen Energy 21 (1996) 465.
[14] S. Cavallaro, N. Mondello, S. Freni, J. Power Sources 102 (2001) 198.
[15] F. Auprêtre, C. Descorme, D. Duprez, Catal. Commun. 3 (2002) 263.
[16] J. Breen, R. Burch, H. Coleman, Appl. Catal. B 39 (2002) 65.
[17] S. Freni, J. Power Sources 93 (2001) 14.
[18] D.K. Liguras, D.I. Kondarides, X.E. Verykios, Appl. Catal. B 43 (2003) 345.
[19] D.K. Liguras, K. Goundani, X.E. Verykios, J. Power Sources, in press.
[20] A.M. Efstathiou, X.E. Verykios, Appl. Catal. A 151 (1997) 109.
[21] E.S. Putna, B. Shereck, R.J. Gorte, Appl. Catal. B 17 (1998) 101.
[22] Z. Zhang, X.E. Verykios, Appl. Catal. A 138 (1996) 109.
[23] V.A. Tsipouriari, X.E. Verykios, J. Catal. 179 (1998) 292.
[24] Z.L. Zhang, X.E. Verykios, Catal. Lett. 38 (1996) 175.
[25] I. Dybkjaer, Fuel Proc. Technol. 42 (1995) 85.
[26] J. Xu, X. Zhang, R. Zenobi, J. Yoshinobu, Z. Xu, J.T. Yates Jr., Surf. Sci. 256 (1991) 288.

[27] Y. Cong, V. van Spaendonk, R.I. Masel, Surf. Sci. 385 (1997) 246.
[28] S.M. Gates, J.N. Russel Jr., J.T. Yates Jr., Surf. Sci. 171 (1986) 111.
[29] M. Guisnet, P. Magnoux, Appl. Catal. A 212 (2001) 83.
[30] B.S. Liu, C.T. Au, Appl. Catal. A 244 (2003) 181.
[31] M.P. Rosynek, R.J. Koprowski, G.N. Dellisante, J. Catal. 122 (1990) 80.
[32] H. Nakano, J. Ogawa, J. Nakamura, Surf. Sci. 514 (2002) 256.
[33] M.C.J. Bradford, M.A. Vannice, Appl. Catal. A 142 (1996) 73.